Transmembrane Topology and Axial Ligands to Hemes in the Cytochrome *b* Subunit of *Bacillus subtilis* Succinate:Menaquinone Reductase†

Cecilia Hägerhäll,‡,§ Henrik Fridén,‡,∥ Roland Aasa,⊥ and Lars Hederstedt*,‡

Department of Microbiology, Lund University, Sölvegatan 21, S-223 62 Lund, Sweden, and Department of Biochemistry and Biophysics, Göteborg University and Chalmers University of Technology, Medicinaregatan 9C, S-41390 Gothenburg, Sweden

Received February 27, 1995; Revised Manuscript Received June 1, 1995⊗

ABSTRACT: The membrane-anchoring subunit of *Bacillus subtilis* succinate:menaquinone reductase is a protein of 202 residues containing two protoheme IX groups with bis-histidine axial ligation. Residues His13, His28, His70, His113, and His155 are the possible heme ligands. The transmembrane topology of this cytochrome was analyzed using fusions to alkaline phosphatase. The results support a proposed model with five transmembrane polypeptide segments and the N-terminus exposed to the cytoplasm. Mutant *B. subtilis* cytochromes containing a His13 → Tyr, a His28 → Tyr, and a His113 → Tyr mutation, respectively, were produced in *Escherichia coli*, partially purified, and analyzed. In addition, succinate:menaquinone reductase containing the His13 → Tyr mutation in the anchor subunit was overproduced in *B. subtilis*, purified, and characterized. The data demonstrate that His13 is not an axial heme ligand. Thermodynamic and spectroscopic properties of the cytochrome are, however, affected by the His13 → Tyr mutation; compared to wild type, the redox potentials of both hemes are negatively shifted and the g_{max} signal in the EPR spectrum of the high-potential heme is shifted from 3.68 to 3.50. From the combined results we conclude that His28 and His113 function as axial ligands to the low-potential heme, which is located in the membrane near the outer surface of the cytoplasmic membrane. Residues His70 and His155 ligate the high-potential heme, which is positioned close to His13 in the protein, near the inner surface of the membrane.

Succinate:quinone reductase (SQR)[1] and quinol:fumarate reductase are membrane-bound respiratory enzyme complexes (EC 1.3.5.1) of conserved composition. They can catalyze the same reactions, although *in vivo* they predominantly function in reverse directions. These enzymes consist of a flavoprotein subunit (FP), containing the dicarboxylate binding site and a covalently bound FAD, and an iron−sulfur protein subunit (IP), containing three iron−sulfur clusters of [2Fe−2S], [4Fe−4S], and [3Fe−4S] types. FP and IP are tightly anchored to the negative side of the membrane, i.e., the inner surface of the bacterial cytoplasmic membrane or the matrix side of the mitochondrial inner membrane, by one or two membrane-spanning polypeptides. For recent reviews see Ackrell et al. (1992) and Hederstedt and Ohnishi (1992). The anchor part is known to be required for quinone reductase/quinol oxidase activity and in most cases it is a cytochrome *b*. The structure and role in enzyme function of this membrane-integral anchor part are not understood.

The anchor subunit of *Bacillus subtilis* SQR is a 23-kDa transmembrane cytochrome b_{558} (Cyt b_{558}) which contains two protoheme IX molecules. One, heme b_H, has a high midpoint potential ($E_{m,7}$ = +16 mV in membrane-bound SQR) and the other, heme b_L, has a low midpoint potential ($E_{m,7}$ = −132 mV in membrane-bound SQR). These two low-spin hemes in Cyt b_{558} also differ in their EPR and optical spectroscopic properties (Hägerhäll et al., 1992).

Heme in the anchor subunit is required for assembly of *B. subtilis* SQR. In the absence of heme, the apocytochrome *b* polypeptide is inserted into the membrane but FP and IP polypeptides, with their prosthetic groups incorporated, accumulate as water-soluble subunits in the cytoplasm (Hederstedt & Rutberg, 1980; Fridén & Hederstedt, 1990). These observations indicate a structural importance of heme in Cyt b_{558}. EPR and near-infrared MCD spectroscopic data, in combination, strongly suggest bis-histidine axial ligation of both hemes in Cyt b_{558} and a near-perpendicular orientation of the two ligating imidazoles at each heme (Fridén et al., 1990).

Cyt b_{558} is not posttranslationally processed at the N-terminal end, except for the removal of the initial methionine from about every second polypeptide (Hederstedt et al., 1987). Hydropathy analysis of the 202-residue-long amino acid sequence of Cyt b_{558} indicates four (Degli-Esposti, 1989; Degli-Esposti et al., 1991) or five (Magnusson et al., 1986; Fridén & Hederstedt, 1990; von Wachenfeldt, 1992) trans-

* Correspondence should be addressed to this author.

† This work was supported by grants from the Swedish Natural Science Research Council, The Swedish Medical Research Council, and the Emil och Wera Cornell's Stiftelse.

‡ Lund University.

§ Present address: Department of Biochemistry and Biophysics, School of Medicine, University of Pennsylvania, Philadelphia, PA 19104-6089.

∥ Present address: Kabi Pharmacia AB, BioScience Center, S-112 87 Stockholm, Sweden.

⊥ Göteborg University and Chalmers University of Technology.

⊗ Abstract published in *Advance ACS Abstracts,* July 15, 1995.

[1] Abbreviations: Cyt b_{558}, cytochrome b_{558}; DCPIP, 2,6-dichlorophenolindophenol; DMN, 2,3-dimethyl-1,4-naphthoquinone; EPR, electron paramagnetic resonance; FP, flavoprotein; HQNO, 2-(*n*-heptyl)-4-hydroxyquinoline *N*-oxide; IP, iron−sulfur protein; MCD, magnetic circular dichroism; MOPS, 3-(*N*-morpholino)propanesulfonic acid; NSMP, nutrient sporulation medium with phosphate; PMS, phenazine methosulfate; QFR, quinol:fumarate reductase; Q_1, 2,3-dimethoxy-5-methyl-6-(3,7-dimethyl-2-butenyl)-1,4-benzoquinone; Q_2, 2,3-dimethoxy-5-methyl-6-(3,7-dimethyl-2,6-octadienyl)-1,4-benzoquinone; SQR, succinate:quinone oxidoreductase.

0006-2960/95/0434-11080$09.00/0

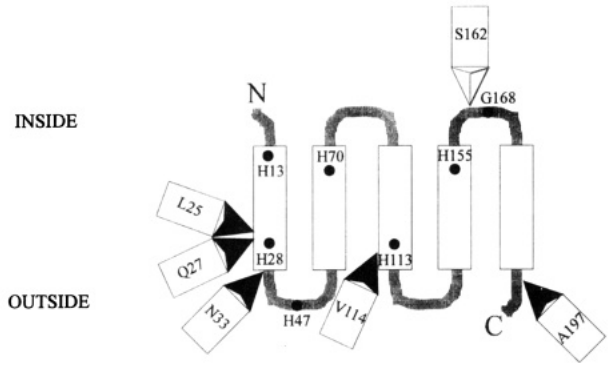

FIGURE 1: Transmembrane topology of the *B. subtilis* Cyt b_{558} (SdhC) polypeptide and an overview on SdhC−PhoA fusions. Inside denotes the cytoplasmic side of the membrane where FP and IP are bound. The SdhC polypeptide contains 202 residues. Residues indicated by dots are histidine (H) residues and a glycine (G) residue that are discussed in the text. The arrows show the position where PhoA is fused in different SdhC−PhoA fusion proteins; the last residue of SdhC in the fusion protein is indicated within the arrow. A black arrowhead indicates fusions that resulted in active alkaline phosphatase (Table 2).

membrane α-helical segments. The distribution of charged amino acids in the polypeptide (the "positive inside" rule; von Heijne, 1986) supports the topology model of Cyt b_{558} with five transmembrane segments shown schematically in Figure 1. In the alternative four-helix model, the hydrophobic segment with residue His155 does not span the membrane and the C-terminus is in the cytoplasm.

The polypeptides of *B. subtilis* SQR are encoded by the *sdhC* (Cyt b_{558}), *sdhA* (FP), and *sdhB* (IP) genes. These genes are organized in a *sdhCAB* operon which has been cloned and sequenced (Magnusson et al., 1986; Phillips et al., 1987). The Cyt b_{558} subunit with normal properties can be synthesized in *Escherichia coli* cells containing the *B. subtilis sdhC* gene, with its native promoter region and ribosome binding sequence, on a multicopy-number plasmid (Magnusson et al., 1985; Hägerhäll et al., 1992). Expression of the *B. subtilis sdhCAB* genes in *E. coli* does not result in an assembled enzyme, and covalently bound FAD is not incorporated into the FP subunit (Hederstedt et al., 1987). *B. subtilis* SQR can, however, be overproduced 3−4-fold in *B. subtilis* containing the *sdhCAB* operon on a low copy-number plasmid (Hägerhäll et al., 1992).

In previous work, the six histidine residues in Cyt b_{558} were individually changed to tyrosines (Fridén & Hederstedt, 1990). The properties of the mutants demonstrated that His13, His28, His47, His70, and His113 can be replaced without total loss of heme from Cyt b_{558}. The His155 → Tyr substitution resulted in a membrane-bound cytochrome polypeptide without heme. It was also shown that cytochrome *b* mutated at His28, His70, His113, or His155 is defective in anchor function, i.e., cannot assemble a membrane-bound SQR. The His47 → Tyr mutation in Cyt b_{558} had no effect on assembly or function of SQR and was therefore excluded as a possible heme ligand. Cytochrome with the His13 → Tyr substitution was found to function as anchor. The assembled SQR with this mutation seemed less active than the wild-type enzyme but was not studied in any detail (Fridén & Hederstedt, 1990).

In the present paper we have experimentally analyzed the topology of the *B. subtilis* Cyt b_{558} polypeptide in the membrane. His → Tyr mutant cytochromes have been analyzed in more detail. Mutant SQR with the His13 → Tyr substitution in Cyt b_{558} was overproduced in *B. subtilis*, isolated, and characterized. From the results we conclude that Cyt b_{558} has five transmembrane segments, that His70 and His155 are the axial ligands to heme b_H, and that His28 and His113 are the axial ligands to heme b_L. This information brings important clues to the possible structure of the membrane-integral part of SQRs and quinol:fumarate reductases.

MATERIALS AND METHODS

Bacterial Strains and Plasmids. Strains and the plasmids used in this work are listed in Tables 1 and 2.

Growth of Bacteria. E. coli strains were grown aerobically at 37 °C in LB medium or on LA plates (Sambrook et al., 1989) supplemented with appropriate antibiotics; ampicillin, 35−50 mg/L; chloramphenicol, 12.5 mg/L; kanamycin, 300 mg/L (used for the selection of clones with *sdhC−phoA* gene fusions). *B. subtilis* strains were grown at 37 °C in nutrient sporulation medium with phosphate (NSMP) (Fortnagel & Freese, 1968) or on minimal salts agar plates (Spizizen, 1958) with 0.5% (w/v) sodium succinate or on tryptose blood agar base plates (TBAB, Difco). Antibiotics were used at the following concentrations for *B. subtilis*: chloramphenicol, 5 mg/L; phleomycin (CAYLA, Toulouse, France), 0.6−1.2 mg/L.

Isolation of sdhC−phoA Fusions. Plasmid pBHH1ΔNH was obtained from pBHHwt (Table 1) by digestion with *Nae*I and *Hin*dIII (Figure 2), treatment with DNA polymerase and dNTP, followed by ligation with T4 DNA ligase. This treatment removed all of *sdhA* from pBHHwt, except for the first 42 bp of the *sdhA* reading frame, but left the *sdh* promoter and the *sdhC* gene intact. CC118/pBHH1ΔNH cells were infected with λTn*pho*-1 (Gutierrez et al., 1987) at a multiplicity of 0.1−1, and transfectants were selected on LA plates supplemented with antibiotics and 5-bromo-4-chloro-3-indolyl phosphate *p*-toluidine (X-phosphate) (40 mg/L) as described by Manoil and Beckwith (1985). Plasmid DNA of PhoA-positive clones was analyzed by cleavage with restriction enzymes, and the *sdhC−phoA* fusion point in selected clones was then determined by DNA sequence analysis using specific oligonucleotide primers. The *sdhC−phoA* fusions were stabilized by subcloning a *Bam*HI−*Xho*I fragment of the plasmids into *Bam*HI- and *Sal*GI-cleaved pUC18, resulting in the pPHO series of plasmids listed in Table 2.

Oligonucleotide-directed deletions within the *sdhC* sequence in the gene fusion present in pPHO197 were constructed using the method of Kunkel et al. (1987) on a *Bam*HI−*Xho*I fragment cloned in M13mp19. *E. coli* RZ1032 was employed for the preparation of uracil-containing single-stranded phage DNA. Two mutagenesis primers were successfully used: fusion point corresponding to residue Val114 (5′TTCGTCAGCTGGCACGCTGACTCTTATA-CACAAG3′) and to residue Ser162 (5′TCGAACGGTT-TATGGTCTGACTCTTATACACAAG3′) in SdhC. Obtained deletions were confirmed by DNA sequence analysis of the entire remaining *sdhC* sequence.

PhoA Fusion Protein Analysis. Alkaline phosphatase activity measurements and immunoblot (Western blot) analysis using PhoA antiserum were done as described by von Wachenfeldt and Hederstedt (1990).

Table 1: Bacterial Strains and Plasmids

strains and plasmids	description	reference or source
	B. subtilis Strains	
3G18	*trpC2 ade met*	G. Venema, University of Groningen
ICD2	*trpC2 met ade ΔsdhCAB::ble*	this work
	E. coli Strains	
CC118	*ΔphoA*	Manoil & Beckwith (1985)
RZ1032	*dut ung*	Kunkel et al. (1987)
LE392	for the propagation of λTn*PhoA*-1	de Bruijn & Lupski (1984)
5K	*hsdM hsdR rpsL thr thiA*	L.-O. Hedén, University of Lund
JM103	*endA1 supE sbcBC thi-1 rpsL Δ(lac−pro) F′ [traD36 lacI^q lacZΔM15 proAB]*	Yanisch-Perron et al. (1985)
JM83	*ara rpsL Δ(lac−proAB) lacZΔM15*	Yanisch-Perron et al. (1985)
	Plasmids	
pHP13	*cat erm*	Haima et al. (1987)
pBluescript KS (−)	*bla*	Stratagene
pUC18	*bla*	Yanisch-Perron et al. (1985)
pBLE-1	*bla ble*	Fridén & Hederstedt (1990)
pSH1047	*kan cat sdhCAB gerE*	Hasnain et al. (1985)
pBSD1200	*cat erm sdhCAB gerE*	Hägerhäll et al. (1992)
pBSD1400	*cat erm sdhCAB*	this work
pBSD1413	*cat erm sdhC5013 sdhAB*	this work
pBHHwt	*bla sdhCA′*	Fridén & Hederstedt (1990)
pBHH1ΔNH	*bla sdhC*	this work
pKIM4	*bla sdhC*	Magnusson et al. (1985)
pTYR13	*bla sdhC5013*	this work
pTYR28	*bla sdhC5028*	this work
pTYR70	*bla sdhC5070*	this work
pKIM116	*tet sdhC113*	Fridén et al. (1987)
pDEL12	*bla ask′*	this work
pBLED34	*bla ble gerE*	this work
pBLED1234	*bla ask′ble gerE*	this work

Table 2: Alkaline Phosphatase Activity of Cells and Cell Fractions of *E. coli* CC118 Containing Plasmids with Different *sdhC−phoA* Gene Fusions[a]

plasmid	fusion point[b]	alkaline phosphatase activity [nmol min^{-1} (mg of protein)$^{-1}$] permeabilized cells	isolated membranes	periplasmic cell fraction
pPHO25	25	22	12	14
pPHO27	27	215	217	70
pPHO33	33	200	224	27
pPHO114	114	235	55	210
pPHO162	162	6	3	4
pPHO197	197	230	700	450
pBHH1ΔNH	negative control	2	1	4

[a] Enzyme activities are the mean of at least two independent experiments. [b] The number is that of the last amino acid residue provided by SdhC in the SdhC−PhoA fusion protein.

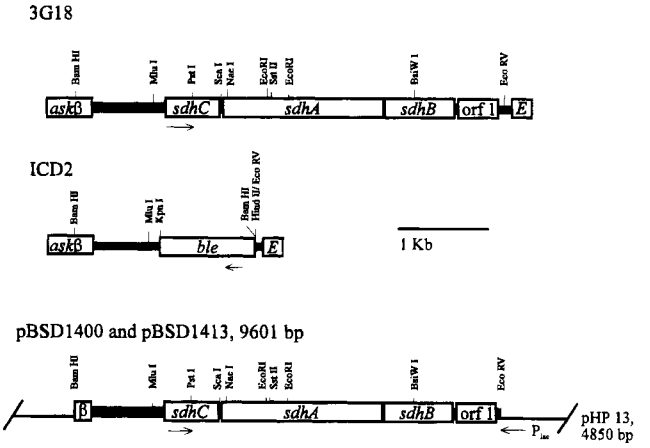

FIGURE 2: Maps of the *sdh* region in the chromosome of *B. subtilis* wild-type strain 3G18 and the *sdh* deletion mutant strain ICD2 and in plasmids pBSD1400 and pBSD1413. In strain ICD2 the *sdhCAB* operon, part of *ask*, and orf1 are deleted and replaced by a *ble* gene conferring phleomycin resistance. The lower part of the figure shows plasmids pBSD1400 and pBSD1413, which are derivatives of plasmid pHP13 and carry the *sdhCAB* genes as a 4.74-kb *Bam*HI−*Eco*RV fragment. pBSD1413 is identical to pBSD1400 except that it contains the *sdhC5013* (His13 → Tyr) mutation. Arrows indicate the direction of transcription of genes. Restriction sites relevant to this work are indicated. *askβ* is the terminal end of the *ask* gene which encodes aspartokinase II. E indicates the *gerE* gene. The orf1 gene encodes a polypeptide of unknown function.

Construction of B. subtilis sdh Deletion Mutant ICD2. Strain ICD2 (Table 1) was obtained by the transformation of *B. subtilis* 3G18 with plasmid pBLED1234 and selection for phleomycin resistance on TBAB plates. The deletion of the *sdhCAB* operon and its replacement by the *ble* gene in the chromosome (Figure 2) was confirmed by Southern blot analysis.

pBLED1234 was obtained as follows. *B. subtilis* DNA flanking the *sdhCAB* operon, i.e., *ask* and *gerE* sequences (Figure 2), were isolated using polymerase chain reaction (PCR) with two pairs of oligonucleotide primers: DEL 1, 5′GGGATTTCAAAAAGGCGGGACTATGCA3′ (contains an *Eco*RI site and corresponds to a sequence in the 3840-bp region of *ask*, Accession No. J03294 and M26384); DEL 2, 5′AAGGTACCCCCTGTTTGATAAGTCC3′ (contains a *Kpn*I site and is complementary to a sequence in the 4600-bp region in the *ask* sequence); DEL 3, 5′GAGGGTCGAC-CTCTTCCGCATGGGAG3′ (corresponds to a sequence at the beginning of orf1 which encodes a putative 17-kDa protein of unknown function, Accession No. M17642); DEL

4, 5′GCTGCAGCGTTCCGTGTCTATTTTC3′ (contains a *Pst*I site and is complementary to a sequence in *gerE*). The primers, DEL 1 + DEL 2 and DEL 3 + DEL 4, were used in two separate PCR reactions with pSH1047 DNA as template, to generate fragments with *ask* and *gerE* sequences, respectively. PCR was performed with *Taq* DNA polymerase (Boehringer Mannheim) in the presence of 1.5 mM $MgCl_2$; 1 min at 94 °C, 2 min at 45 °C, and 3 min at 72 °C in a total of 25 cycles. The DEL 1/DEL 2 product (*ask′*) was cleaved with *Eco*RI and *Kpn*I and then cloned into pUC18, resulting in pDEL12. The DEL 3/DEL 4 product (*gerE′*) was cleaved with *Eco*RV and *Pst*I and ligated to pBLE1 cleaved with *Hin*dII and *Pst*I, resulting in pBLED34. Finally, the *Eco*RI−*Kpn*I fragment of pDEL12 was cloned into pBLED34 cleaved with the same two enzymes. The resulting plasmid, pBLED1234, contains the phleomycin resistance gene, *ble*, flanked by a 0.8-kb *ask′* and a 1.0-kb *gerE′* fragment. The *ble* and *gerE′* sequences in pBLED1234 are transcribed from opposite DNA strands.

Construction of the pTYR Series of Plasmids. The previously constructed set of plasmids with mutant *B. subtilis sdhC* genes corresponding to the His13 → Tyr (*sdhC5013*), His28 → Tyr (*sdhC5028*), and His70 → Tyr (*sdhC5070*) mutations in Cyt b_{558} are derivatives of pUC19. These plasmids contain a *sdh* promoter mutation which has a small effect on *sdhC* gene expression in *E. coli* but severely decreases gene expression in *B. subtilis* (Fridén and Hederstedt, 1990). To eliminate the promoter-down mutation, we constructed plasmids pTYR13 (*sdhC5013*), pTYR28 (*sdhC5028*), and pTYR70 (*sdhC5070*). These plasmids were obtained after oligonucleotide-directed mutagenesis of the *Bam*HI−*Pst*I *B. subtilis sdhC* subfragment from pSH1047 cloned in phage M13 mp18 essentially as described before (Fridén & Hederstedt, 1990) except that the method of Kunkel et al. (1987) was employed to select for desired clones. The *Mlu*I−*Pst*I fragment of the wild-type *sdhC* gene in pKIM4 (Figure 2) was then replaced by this fragment from the different mutant *sdhC* genes. Nucleotide sequence analysis of the *sdh* promoter region and the *sdhC* gene of the resulting plasmids, pTYR13, pTYR28, and pTYR70, confirmed the identity to pKIM4 except for the respective site-specific *sdhC* mutation. Plasmids pKIM4 and pKIM116 are derivatives of pBR322 containing the *B. subtilis* wild-type *sdhC* gene and a mutant *sdhC* gene (corresponding to the His113 → Tyr mutation in Cyt b_{558}), respectively, on a *Bam*HI−*Eco*RI fragment (Table 1). The *sdhC* gene in these plasmids is flanked by a 1-kb fragment containing the *sdh* promoter region and a 0.5-kb fragment containing the first part of *sdhA*.

Construction of pBSD1400 and pBSD1413. Plasmids pBSD1400 and pBSD1413 (Figure 2), used for the overproduction of wild-type and mutant SQR in *B. subtilis* strain ICD2, were constructed in the following way. A 4.7-kb *Bam*HI−*Eco*RV fragment carrying *sdhCAB* was isolated from pSH1047 (Table 1) and ligated to pBluescript KS(−) treated with shrimp alkaline phosphatase (U.S. Biochemical Corp.). The resulting plasmid, pBLUES3, was cleaved with *Bam*HI and *Sal*I, and the fragment containing *sdh* genes was ligated to cleaved and phosphatase-treated pHP13. This plasmid was called pBSD1400 (Figure 2). Plasmid pBSD1413 was obtained by replacing the *Mlu*I−*Sca*I fragment (carries *sdhC*) in pBSD1400 with the corresponding fragment isolated from pTYR13. pBSD1400, pBSD1413, and pHP13 were introduced into strain ICD2 by protoplast transformation (Hoch, 1991).

Purification of Wild-Type and Mutant Cytochrome Subunit from E. coli. Membranes from *E. coli* 5K containing pKIM4, pTYR13, pTYR28, or pKIM116 were prepared from cells grown in LB with 0.5% glucose and 35 mg/L ampicillin (Fridén, et al., 1990). Cyt b_{558} was isolated after solubilization of the membrane with non-ionic detergent as described before (Fridén et al., 1990), but Triton X-100 was replaced by Thesit (Boehringer Mannheim) of the same concentration.

Purification of Mutant SQR. Membranes from *B. subtilis* ICD2 containing pBSD1400, pBSD1413, or pHP13 were isolated from cells grown in NSMP as described before (Hederstedt, 1986). Mutant SQR with the His13 → Tyr mutation in Cyt b_{558} was isolated from membranes of strain ICD2/pBSD1413 using the same protocol as for the wild-type enzyme (Hägerhäll et al., 1992).

Miscellaneous Methods. Succinate oxidase activity was measured at 30 °C in 20 mM Na-MOPS/HCl buffer pH 7.5 containing 10 mM potassium phosphate and 10 mM potassium succinate using a Clark-type oxygen electrode. Other enzyme activity measurements, low-temperature optical spectroscopy, EPR spectroscopy, spin quantitation of the [2Fe−2S] cluster, redox titrations, rocket immunoelectrophoresis, protein determination, and heme determination as pyridine hemochromogen were all done as recently described (Hägerhäll et al., 1992). General recombinant DNA techniques, including Southern blot and PCR, were done as described in Sambrook et al. (1989). DNA fragments were isolated from agarose gels using Geneclean (BIO 101 Inc., La Jolla, CA). DNA sequence analysis was done by the dideoxy chain-termination method with the Sequenase II kit and [^{35}S]dATP (USB/Amersham).

RESULTS

Cytochrome b−Alkaline Phosphatase Fusions. To analyze the transmembrane topology of the Cyt b_{558} polypeptide, we made used of the *phoA* gene fusion system developed by Manoil and Beckwith [for review see Manoil et al., (1990)]. The reliability of this system to determine topologies of membrane proteins is well documented by, for example, its application on the L-subunit of the bacterial photosynthetic reaction center for which the structure is known (Yun et al., 1991). The system is based on the fact that *E. coli* alkaline phosphatase (PhoA) polypeptide requires a N-terminal signal sequence in order to be transported from the cytoplasm, where it is synthesized, across the cytoplasmic membrane to the periplasm. Intramolecular disulfide bonds are required for PhoA to be enzymatically active. These bonds cannot be made in the cytoplasm but form in the periplasm, promoted by the activity of a periplasmic protein disulfide isomerase, DsbA [cf. Creighton and Freeman (1993)].

A first generation of *sdhC−phoA* fusions were selected *in vivo* in *E. coli* CC118/pBHH1ΔNH using bacteriophage λTn*phoA*-1. Strain CC118 is deleted for the *phoA* gene in the chromosome and plasmid pBHH1ΔNH carries the *B. subtilis sdhC* gene which is expressed in *E. coli*. Phage λTn*phoA*-1 contains a transposon into which has been inserted a modified *phoA* gene encoding a PhoA polypeptide variant without the signal sequence needed for export of the protein (Gutierrez et al., 1987). A transmembrane segment of a membrane protein can substitute for the lacking export

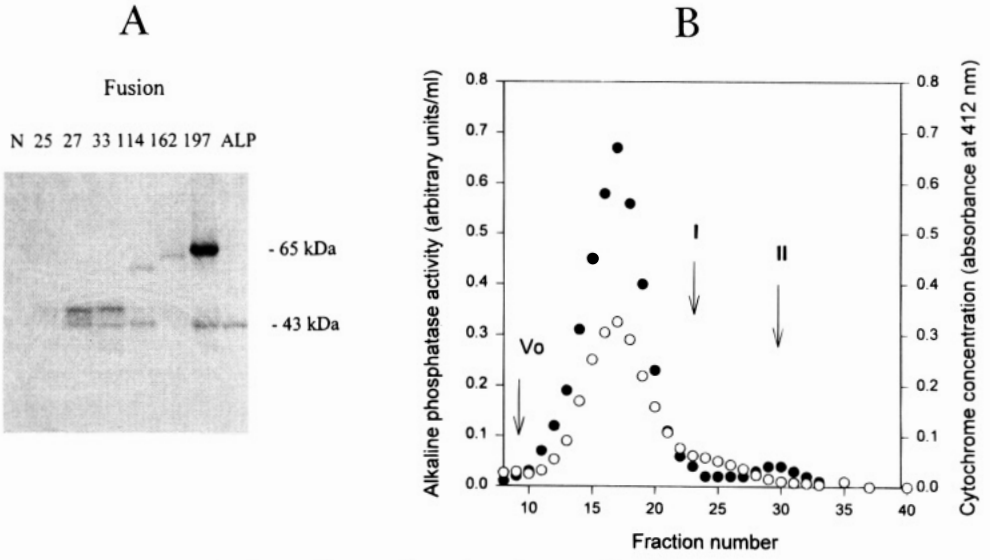

FIGURE 3: (A) SdhC−PhoA fusion protein in membranes. Shown is an immunoblot of isolated membranes from *E. coli* CC118 containing the different plasmids presented in Table 2. Membrane polypeptides (5 μg of protein) and, as a reference, 50 ng of purified PhoA (ALP) were separated by SDS−polyacrylamide electrophoresis in a 7.5−12% (w/v) acrylamide gradient gel, electroblotted to a nitrocellulose filter, and probed with antiserum against *E. coli* PhoA protein. The numbers indicated for the different lanes correspond to the fusion point in the fusion proteins. Negative control (N) is membranes from CC118/pBHH1ΔNH. (B) Gel filtration of the SdhC−PhoA fusion protein which contains 197 residues of Cyt b_{558}. Membrane proteins of *E. coli* CC118/pPHO197 were solubilized in Triton X-100 and size-fractionated in the presence of 0.05% (w/v) detergent on a Sephacryl S-300 column as described by Fridén et al. (1990). Fractions were analyzed for alkaline phosphatase activity (filled symbols) and cytochrome *b* (open symbols). The arrows V_o, I and II, indicate the void volume, the position where wild-type Cyt b_{558} is eluted, and the position where wild-type (not fused) *E. coli* soluble alkaline phosphatase is eluted, respectively.

signal sequence if it is fused with the mutant PhoA protein. Hence, a *sdhC−phoA* in frame fusion in plasmid pBHH1ΔNH in a region corresponding to a Cyt b_{558} polypeptide segment located on the periplasmic (positive) side of the membrane is expected to give a PhoA-positive phenotype to *E. coli* strain CC118. Such clones can be discriminated from PhoA-negative clones by the color of colonies on zymochromogenic (X-phosphate) plates. DNA sequence analysis of nine clones with *sdhC−phoA* fusions, isolated in independent screenings, identified four different fusions. The positions of the fusion to PhoA in these clones correspond to the residues immediately following Leu25, Glu27, and Asp33, respectively, at the end of the first predicted transmembrane segment in the cytochrome polypeptide and that following Ala197 close to the C-terminal end of the Cyt b_{558} polypeptide (Figure 1). The *sdhC−phoA* gene fusions in the original isolates were stabilized by subcloning them into pUC19 resulting in the series of plasmids presented in Table 2. The subcloning eliminated transposase functions and the kanamycin resistance gene of λTn*phoA*-1.

To probe the topology of the middle part of the Cyt b_{558} polypeptide, a second generation of fusions were constructed *in vitro* by oligonucleotide-directed deletion mutagenesis. The *sdhC−phoA* fusion in pPHO197 (encoding the C-terminal fusion) was used to construct hybrids corresponding to fusion proteins where PhoA immediately follows residue Val114 and Ser162, respectively, in Cyt b_{558}. Attempts to obtain a variant with a fusion next to Ala85 in the cytochrome were unsuccessful.

The amount of exported active PhoA resulting from the different gene fusions in *E. coli* CC118 was analyzed by alkaline phosphatase activity measurements with permeabilized cells (Table 2). The subcellular localization of active PhoA was determined by activity measurements with periplasmic and membrane cell fractions (Table 2). Figure 3A shows the size and relative amount of membrane-bound fusion protein obtained from the different plasmid-borne *sdhC−phoA* gene fusions as determined by immunoblot (Western blot) using antiserum against PhoA. All fusion proteins were membrane-bound and of expected sizes.

The results of the SdhC−PhoA fusion analysis fully support the transmembrane topology of Cyt b_{558} shown in Figure 1. Fusions at the C-terminal end of the first, third, or fifth predicted transmembrane segment resulted in exported active PhoA, whereas a fusion at the C-terminal end of the fourth predicted transmembrane segment resulted in inactive PhoA. The presence of membrane-bound Ser162 fusion protein excluded the possibility that this clone was inactive due to lack of enzyme protein. Several clones contained membrane-bound 43-kDa PhoA antigen which probably corresponds to the very stable PhoA domain and was derived from proteolytic processing of fusion protein. This 43-kDa PhoA antigen was not detected in membranes containing the Leu25 or Ser162 fusion proteins. The membrane-bound Leu25 fusion protein, with only the first 25 residues of SdhC fused to PhoA, seemingly has the fusion point located inside the hydrophobic core of the membrane (Figure 1) and for this reason may not be accessible to proteolytic cleavage. The membrane-bound Ser162 fusion protein has the PhoA domain in the cytoplasm and thus does not contain the intramolecular disulfide bridges required for enzyme activity. The Ser162 protein is for this reason probably very prone to degradation and this may explain the lack of detectable amounts of 43-kDa PhoA antigen in *E.coli* CC118/pPHO162.

Light Absorption Difference (Dithionite-Reduced minus Oxidized) Spectra of E. coli. CC118/pPHO197 membranes (contain the Ala197 fusion protein) and CC118/pBHH1ΔNH membranes (contain wild-type Cytb_{558}) showed elevated amounts of cytochrome *b* as compared to those of CC118

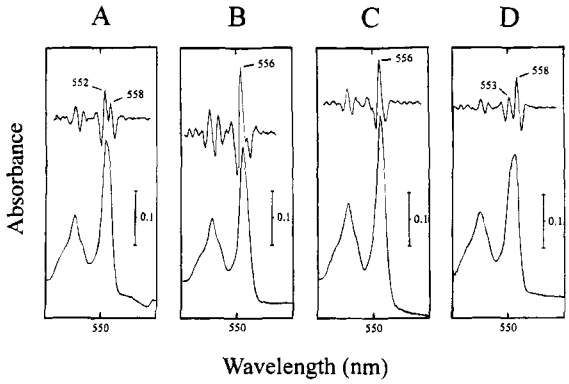

FIGURE 4: Low-temperature light absorption spectra of isolated wild-type and mutant Cyt b_{558}. Shown are 77 K difference (dithionite-reduced minus oxidized) spectra of His13 → Tyr (A), His28 → Tyr (B), and His113 → Tyr (C) mutant cytochromes and that of wild-type (D) *B. subtilis* Cyt b_{558} produced in *E. coli* and purified to spectral homogeneity. The fourth derivatives of the spectra are shown in the upper part of the panels. The vertical bars indicate the absorption scale and the wavelength span shown is 500−600 nm.

containing pPHO25, pPHO27, pPHO33, pPHO114, pPHO162, or pUC19 (spectra not shown). The α-band peak in the 77 K difference absorption spectrum of CC118/pPHO197 membranes showed the split characteristic for wild-type *B. subtilis* Cyt b_{558}. Membrane proteins of CC118/pPHO197 were solubilized using Triton X-100 and fractionated on a gel-filtration column in the presence of the detergent (Figure 3B). Alkaline phosphatase activity, the 65-kDa Ala197 fusion protein (determined as PhoA antigen in immunoblots; data not shown) and the Cyt b_{558} chromophore (assayed by the absorption at 412 nm and confirmed by light absorption spectra) coeluted. The fusion protein eluted in fractions corresponding to a molecular size which is larger than that of wild-type Cyt b_{558} bound to detergent micelles and much larger than *E. coli* alkaline phosphatase (86-kDa water-soluble homodimer). The cytochrome was precipitated using antiserum against PhoA (not shown). These results demonstrate that the Ala197 fusion protein contains heme and has spectral properties similar to wild-type Cyt b_{558}. This strongly suggests that the transmembrane topology of the SdhC part is normal in the membrane-bound fusion protein.

Purification and Properties of Mutant Cyt b_{558}. Cytochrome with the His13 → Tyr, His28 → Tyr, His70 → Tyr, or His113 → Tyr mutation was produced in *E. coli* 5K containing plasmid pTYR13, pTYR28, pTYR70, or pKIM116, respectively. Wild-type Cytb_{558} was produced in *E. coli* 5K containing plasmid pKIM4. The yield of mutant cytochromes was in all cases lower than for the wild type despite the fact that all the plasmids were identical except for a single missense mutation in *sdhC*. Very low amounts of the His70 → Tyr mutant protein was obtained in strain 5K/pTYR70 and this variant was not further analyzed. Cyt b_{558} was solubilized from membranes of all the other strains using the nonionic detergent Thesit and partially purified by gel-filtration chromatography in the presence of 0.05% (w/v) Thesit.

Reduced heme b_H and b_L in wild-type Cyt b_{558} show a symmetrical (555 nm) and a split (552 and 558 nm) α-band peak, respectively, in 77 K light absorption spectra (Hägerhäll et al., 1992). Figure 4 shows low-temperature light absorption spectra of mutant and wild-type Cyt b_{558}. Dithionite-reduced His13 → Tyr mutant cytochrome showed a split α-band absorption peak similar to wild type, but the shape of the peak was not the same (compare Figure 4, panels A and D). The spectrum of isolated wild-type Cyt b_{558} shows a shoulder on the "blue" side of the peak, whereas that of the mutant cytochrome had the shoulder on the "red" side. The His28 → Tyr and His113 → Tyr mutant cytochromes reduced by dithionite showed essentially symmetrical α-band peaks with the absorption maximum at about 556 nm (Figure 4B,C), i.e., showed spectra similar to that of heme b_H in wild-type cytochrome. Redox titrations of the partially purified His28 → Tyr mutant cytochrome demonstrated a single n = 1 component with a midpoint potential of +40 ± 10 mV at pH 7.4 (not shown).

Membrane-Bound SQR Containing His13 → Tyr Mutant Cytochrome. To produce SQR with the His13 → Tyr mutation in Cyt b_{558}, plasmid pBSD1413 and *B. subtilis* strain ICD2 were constructed as described in Materials and Methods. Strain ICD2 has the entire *sdhCAB* operon deleted from the chromosome and replaced by a phleomycin resistance gene (Figure 2). pBSD1413 (encoding the mutant enzyme), pBSD1400 (encoding the wild-type enzyme), and pHP13 (vector only) were introduced into strain ICD2 by protoplast transformation. Transformants were selected on rich medium containing chloramphenicol. The strains ICD2/pBSD1400 and ICD2/pBSD1413, but as expected not ICD2/pHP13, were found to grow on minimal succinate medium. This demonstrated that the mutant SQR encoded by pBSD1413 is functional.

Membranes were isolated from the three strains grown in NSMP supplemented with chloramphenicol and harvested at the end of exponential growth phase. The concentration of both SQR polypeptide and heme in ICD2/pBSD1413 membranes was about half compared to that in ICD2/pBSD1400 membranes (Table 3). However, whole-cell lysates of ICD2/pBSD1400 and ICD2/pBSD1413 contained about the same amount of FP antigen, as determined by rocket immunoelectrophoresis, which shows that the *sdhCAB* operon is expressed to a similar extent in the two strains. These observations suggest that the His13 → Tyr mutant cytochrome is synthesized in lower amounts or is less stable than the wild-type cytochrome.

Redox titrations of the mutant SQR in ICD2/pBSD1413 membranes showed two n = 1 components corresponding to the two heme groups in cyt b_{558} (Figure 5). The midpoint potential of heme b_H was found to be shifted by −89 mV relative to that of wild type. That of heme b_L was also shifted, but only by −35 mV. The contribution of heme b_H to the maximal absorption at 558 nm (of the fully reduced cytochrome) was lower, about 40% in the mutant compared to 50% in the wild type.

The apparent turnover number of SQR containing the His13 → Tyr mutation in Cyt b_{558}, measured with PMS or Q_1 as electron acceptor, was about 50% compared to wild type (Table 3). The succinate oxidase activity (rate of dioxygen consumption per SQR molecule in the membrane) of ICD2/pBSD1400 and ICD2/pBSD1413 membranes were the same, 0.8 s^{-1}, indicating that SQR activity in these membranes is not a rate-limiting step in respiration with succinate. This agrees with the similar growth rates of ICD2/pBSD1400 and ICD2/pBSD1413 on plates and in liquid media.

Table 3: Composition and SQR Enzyme Activity of Membranes from Different *B. subtilis* Strains

membrane	SQR	concentration[a] (nmol/mg of protein) protoheme IX	FP	FAD	SQR activity[b] [μmol of succinate oxidized min^{-1} (mg protein)$^{-1}$] PMS	Q_1	SQR activity[b] [mol of succinate oxidized (mol of SQR)$^{-1}$ s^{-1}] PMS	Q_1
ICD2/pBSD1400	wild type	2.9	1.6	1.5	4.8	1.5	50	16
ICD2/pBSD1413	His13 Cyt *b* mutant	1.5	0.88	0.82	1.5	0.4	29	8
ICD2/pHP13	absent	0.2	nd[c]	nd	nd	nd		

[a] Protoheme IX was determined as the pyridine hemochromogen. FP was determined as antigen by rocket-immunoelectrophoresis. FAD was determined as covalently bound FAD. The results are from duplicate analyses of two independent membrane preparations from each strain. The difference in results between the duplicate analyses of the same preparation was less than 10%. [b] Enzyme activities were determined at 30 °C using DCPIP as final electron acceptor. [c] nd, not detectable.

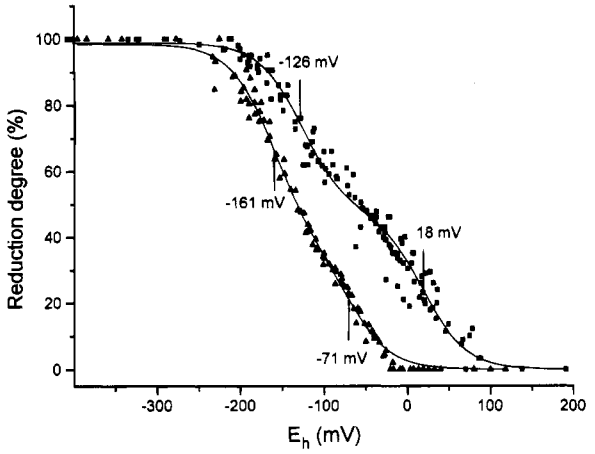

FIGURE 5: Potentiometric analysis of Cyt b_{558} in membrane-bound wild-type and mutant SQR. Redox titrations using mediator dyes were performed at pH 7.4 with ICD/pBSD1400 membranes (squares) containing wild-type SQR and on ICD2/pBSD1413 membranes (triangles) containing SQR with the His13 → Tyr mutant cytochrome. The midpoint potentials, +18 and −126 mV for the hemes in the wild-type enzyme and −71 and −161 mV for those in the mutant enzyme, were obtained from the data fitted to the Nernst equation with two $n = 1$ components.

Properties of Purified Mutant SQR. SQR with the His13 → Tyr mutation in the cytochrome subunit was solubilized from ICD2/pBSD1413 membranes using Thesit and purified to homogeneity following the same protocol as previously used for wild-type enzyme (Hägerhäll et al., 1992). The yield of pure enzyme from membranes was about 15% of the maximal theoretical value. As shown in Table 4, purified mutant SQR contained 2 mol of protoheme IX/mol of enzyme protein and covalently bound FAD. The isolated mutant SQR was about half as active as that of wild type, regardless of whether PMS, quinones, or quinols were used as electron acceptors/donors (Table 5). Both the succinate: quinone reductase and the quinol:fumarate reductase activities of the mutant SQR were sensitive to 2-(*n*-heptyl)-4-hydroxyquinoline *N*-oxide (HQNO) (Table 5). The apparent K_i for HQNO of mutant and wild-type enzyme in the membrane were the same, 0.4 μM, as determined using Q_1 as electron acceptor.

The isolated mutant SQR was stable for several weeks when stored in the oxidized state at 0 °C. Reduced with succinate or dithionite, it showed a pronounced instability which is in contrast to the membrane-bound mutant enzyme and isolated wild-type SQR (Hägerhäll et al., 1992). For example, incubation of the isolated mutant SQR at 30 °C, pH 7.4, in the presence of 10 mM succinate resulted in the loss of 7−9% of the activity/min (measured with PMS as electron acceptor). Reliable redox titrations with the isolated mutant SQR could not be performed due to this instability of the reduced enzyme. Instability in the mutant cytochrome in isolated enzyme was also indicated by increased reactivity of the dithionite-reduced enzyme with carbon monoxide, as determined by spectroscopy and compared to isolated wild-type enzyme.

Mutant and wild-type SQR showed differences in the absorptivity of Cyt b_{558} (Table 4). The difference (reduced minus oxidized) extinction coefficient for the Soret peak (428 minus 411 nm) was higher in the mutant, whereas that of the α-band peak (558 minus 575 nm) was lower. This lower extinction coefficient for the α-band peak of the mutant enzyme explains the smaller than wild-type contribution of heme b_H in redox titrations of the membrane-bound mutant SQR (Figure 5). The 77 K light absorption difference (dithionite-reduced minus oxidized) spectrum of purified mutant SQR was similar but not identical to that of wild type (spectra not shown). The shoulder of the asymmetric (split) α-band absorption peak is seen on the "blue" side in the case of the mutant enzyme but on the "red" side for the wild-type SQR. Thus, the low-temperature spectrum of the His13 → Tyr mutant cytochrome in assembled SQR resembles the spectrum of isolated wild-type Cyt b_{558} and vice versa.

EPR spectra of purified mutant SQR in the oxidized state showed two low-spin heme signals (Figure 6). The g_{max} of the signal of the, at pH 7.4, succinate-reducible heme, b_H, was at $g = 3.50$ for the mutant and $g = 3.68$ for the wild type (Hägerhäll et al., 1992). That of heme b_L was in the mutant at $g = 3.39$, which is close to that of wild-type SQR ($g = 3.42$). The EPR spectra and the redox midpoint potentials of the three iron−sulfur clusters are normal in membrane-bound SQR with the His13 → Tyr mutation in Cyt b_{558} (C. Hägerhäll, V. Sled', and T. Ohnishi, unpublished data).

DISCUSSION

Transmembrane Topology of Cyt b_{558}. The amino acid sequence of the FP and IP subunits, and the set of prosthetic groups present in these proteins, are very conserved when succinate:quinone oxidoreductases from different organisms are compared. In contrast, the anchor subunit shows little sequence conservation and the composition varies depending on the organism. It can consist of one longer hydrophobic polypeptide containing two protoheme IX molecules, as in the cases of *B. subtilis* SQR and *Wolinella succinogenes* quinol:fumarate reductase. The anchors of *E. coli* and mammalian SQR consist of two polypeptides and one heme,

Table 4: Chemical Composition and Properties of Purified Wild-Type SQR and Mutant SQR with the His13 → Tyr Mutation in Cyt b_{558}

composition or property[a]	wild-type SQR	mutant SQR
ratio protoheme IX/[2Fe−2S] (mol/mol)	2.0	2.1
ratio FP/[2Fe−2S] (mol/mol)	1.0	1.2
EPR low-spin heme signals (g_{max})	heme b_H; $g = 3.68$ heme b_L; $g = 3.42$	heme b_H; $g = 3.50$ heme bL; $g = 3.39$
succinate reducibility of cytochrome at pH 7.4 (%)	60	35
ϵ of dithionite-reduced enzyme (558 nm minus 575 nm) (mM^{-1} cm^{-1})	45	33
ϵ of dithionite-reduced enzyme (428 nm minus 411 nm) (mM^{-1} cm^{-1})	269	370

[a] FP was determined as antigen, [2Fe−2S] was quantitated by EPR, and protoheme IX was determined as the pyridine hemochromogen. Succinate reducibility was calculated from the absorption at 558 nm minus that at 575 nm obtained in the presence of 10 mM succinate compared to that obtained by dithionite.

Table 5: Enzyme Activities of Purified *B. subtilis* Mutant SQR with the His13 → Tyr Mutation in Cyt b_{558}

	succinate:quinone reductase activity[b] (s^{-1})			
additions[a]	activity using DCPIP as electron acceptor[c]		activity with quinone as the only electron acceptor or donor[d]	
none	8.6	(61%)		
+ PMS	69	(59%)		
+ PMS + HQNO	72	(65%)		
+ Q_1	14	(36%)	5.6	(31%)
+ Q_1 + HQNO	3.5	(70%)	0.6	(30%)
+ Q_2	16	(33%)	6.2	(33%)
+ Q_2 + HQNO	3.0	(42%)	0.7	(35%)
+ $DMNH_2$			15	(48%)
+ $DMNH_2$ + HQNO			2.2	(147%)

[a] The temperature was 30 °C and the final concentration in the cuvette of added compounds were as follows: succinate, 20 mM; fumarate, 10 mM; DCPIP, 20 μg/mL; PMS, 0.5 mg/mL; HQNO, 10 μM; Q_1 or Q_2, 50 μM in the DCPIP assay and 200 μM in the absence of DCPIP; $DMNH_2$, 200 μM. [b] Percentage of activity compared to purified wild-type *B. subtilis* SQR is given within the parentheses. [c] Succinate:DCPIP reductase activity under aerobic conditions. [d] Succinate:quinone reductase or quinol:fumarate activities under anaerobic (cuvette evacuated and flushed with nitrogen gas) conditions.

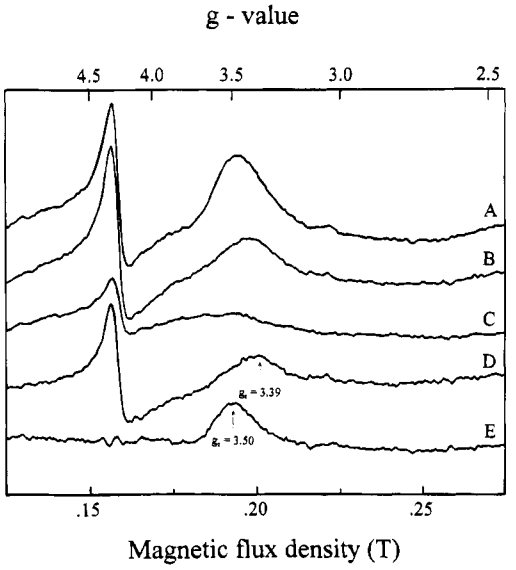

FIGURE 6: EPR spectra of isolated SQR with the His13 → Tyr mutation in Cyt b_{558}. Trace A, oxidized enzyme; trace B, succinate-(20 mM) reduced enzyme; trace C, dithionite-reduced enzyme; trace D, difference spectrum B minus C (shows b_L); trace E, difference spectrum A minus B (shows b_H). The enzyme concentration was 90 μM. Experimental conditions: microwave frequency, 9.445 GHz; power, 2 mW; modulation amplitude, 2 mT; temperature, 11 K. The corresponding EPR spectra of wild-type SQR are shown in Hägerhäll et al. (1992).

whereas *E. coli* quinol:fumarate reductase contains two anchor polypeptides but no heme. In the cases of mammalian mitochondrial SQR and *B. subtilis* SQR, it has been demonstrated that the membrane anchor spans the mitochondrial inner membrane and the bacterial cytoplasmic membrane, respectively [for reviews see Ackrell et al. (1992) and Hederstedt and Ohnishi (1992)]. Hydropathy analyses of the sequences for anchor polypeptides show a conserved pattern of five hydrophobic stretches in the single-polypeptide anchors and three such stretches in each polypeptide in anchors with two polypeptides. These hydrophobic stretches are assumed to be transmembrane segments, but this had not been analyzed experimentally.

Using alkaline phosphatase (PhoA) fused at the C-terminal end to various truncated variants of the *B. subtilis* Cyt b_{558} polypeptide, we have in this work confirmed a proposed topology model for the protein with five transmembrane segments and the N-terminus exposed on the cytoplasmic side of the membrane (Figure 1). The model is further supported by the observation that a Gly168→Asp mutation in Cyt b_{558} makes FP and IP unable to bind to the cytochrome but does not affect the light absorption spectrum (Fridén et al., 1987). This agrees with the location of Gly168 in a hydrophilic loop exposed to the cytoplasm (Figure 1).

Identification of Residues Serving as Heme Axial Ligands in Cyt b_{558}. Four histidine residues serve as axial ligands to the two protoheme IX molecules in Cyt b_{558} (Fridén et al., 1990). All the histidines in *B. subtilis* Cyt b_{558}, except the dispensable His47, are located in hydrophobic segments. In the topology model (Figure 1), residues His13, His70, and His155 are located close to the cytoplasmic side of the membrane, whereas residues His28 and His113 are closer to the outer side of the membrane. This arrangement indicates that His28 and His113 could be the axial ligands to one heme and two of residues His13, His70, and His155 could be the axial ligands to the other heme, assuming a perpendicular orientation of the heme planes relative to the membrane plane, as is the case in other integral membrane-bound cytochromes *b* (Bergström, 1985; Salerno & Ingledew, 1991; Ingledew et al., 1992). For the single-heme anchor of bovine heart and *Saccharomyces cerevisiae* mitochondrial SQR, it has been suggested on the basis of sequence comparisons that two histidine residues in one of the anchor polypeptides, corresponding to His13 and His70 in *B. subtilis*

Cyt b_{558}, function as axial heme ligands (Yu et al., 1992; Daignan-Fornier et al., 1994). Mutant data with *E. coli* SQR suggest that the axial heme ligands are two residues of those corresponding to His13, His 70, and His155 in *B. subtilis* Cyt b_{558} [C. Vibat and R. B. Gennis, unpublished data quoted in Hederstedt and Ohnishi (1992)]. To identify the histidine residues which function as axial heme ligands in SQR we analyzed mutant *B. subtilis* Cyt b_{558}.

Cyt b_{558} with the His13 → Tyr mutation was found to be functional, and like wild-type cytochrome it contains two low-spin heme groups with different spectral and thermodynamic properties (Figures 5 and 6 and Table 4). From these data we conclude that His13 cannot be important for heme ligation. Consequently His28, His70, His113, and His 155 are the axial heme ligands in *B. subtilis* Cyt b_{558}. Extrapolated to anchors of other SQRs on the basis of sequence similarities, our results indicate that the His residue at position 90 in the QPs1/C_{II-3} anchor polypeptide of bovine SQR (Yu et al., 1992) (position 98 in the revised sequence; Cochran et al., 1994), at position 156 in the SDH3/CYB3 polypeptide of *S. cerevisiae* SQR (Abraham et al., 1994; Daignan-Fornier et al., 1994), and at position 29 in the SdhC polypeptide of *E. coli* SQR (Wood et al., 1984) are not axial heme ligands.

Which Pair of Residues Ligates Heme b_H and Heme b_L, Respectively? Sequence comparisons between *B. subtilis* Cyt b_{558} and anchors of other SQRs and quinol:fumarate reductases further show, despite the overall low sequence similarity, that those anchor proteins with only one heme consistently contain the histidine residues corresponding to *B. subtilis* His70 and His155 but lack both of those corresponding to His28 and His113 (Hägerhäll, 1994). This observation strongly suggests that His70 and H155 act as ligands to the same heme in *B. subtilis* Cyt b_{558}.

Our results with isolated mutant Cyt b_{558} containing the His28 → Tyr or the His113 → Tyr mutation indicate that they have both lost heme b_L. One interpretation of this is that His28 and His113 are the axial ligands to heme b_L. However, the properties of the mutant cytochromes could be misleading since the loss of one heme may change the properties of the remaining heme.

EPR spectroscopy of isolated *B. subtilis* SQR with the His13 → Tyr mutation in Cyt b_{558} showed that heme b_H is significantly affected by the mutation, i.e., g_{max} is shifted from 3.7 to 3.5. The EPR signals of heme b_L and the three iron−sulfur clusters were found to be normal in the mutant. This specific effect on the EPR spectrum of the iron in heme b_H is most likely caused by a structural change in the local environment of that heme. Other indications of a slight structural change in the mutant SQR were enzyme instability, reactivity of the reduced cytochrome with carbon monoxide, and the altered optical spectrum. The midpoint redox potential of heme b_H and heme b_L in the membrane-bound His13 → Tyr mutant SQR relative to wild type was found to be shifted from $+18 \pm 3$ to -71 ± 4 mV and from -126 ± 3 to -161 ± 3 mV, respectively. The low redox potential of heme b_H in the mutant Cyt b_{558} is, as for the EPR signal, most likely an effect of a local structural change in the vicinity of this heme. The small negative shift in the potential of heme b_L is probably not resulting from a structural change in the environment of this heme since the EPR signal was essentially unaffected. We interpret the small shift in midpoint potential of heme b_L as being a consequence of the negative shift in potential of heme b_H, i.e., an effect of negative cooperativity between the two close heme groups in Cyt b_{558}. Such anticooperativity has been described in other systems (Robertson et al., 1994) and is consistent with the observation that the midpoint potential of heme b_L in *B. subtilis* SQR, can be shifted −55 mV without effect on the redox potential of heme b_H (Smirnova et al., 1995). The role of heme in SQR for electron transfer from succinate to quinone is not known. The turnover of the mutant enzyme was about half compared to wild type. From the available data it cannot be concluded whether this reduced enzyme activity is a direct structural effect of the His13 → Tyr mutation or an indirect effect of the lower redox midpoint potential of the hemes.

On the basis of the topology data (this work), mutant data (Fridén et al., 1987; Fridén & Hederstedt, 1990; this work); and sequence comparisons, we have proposed a three-dimensional structural model for the integral membrane part of Cyt b_{558} in *B. subtilis* SQR (Hägerhäll, 1994; Hägerhäll and Hederstedt, manuscript in preparation). In this model, the first four transmembrane segments of Cyt b_{558} constitute an antiparallel four-helix bundle which harbors both hemes. Each α-helical transmembrane segment in the bundle carries one axial ligand to heme iron and this "locks" the relative orientation of the four helices, i.e., they cannot be rotated. In the proposed structure, His13 faces the interior of the bundle and is close to the heme ligated by His70 and His155. Since the His13 → Tyr mutation dominantly affects the high-potential heme, we conclude in agreement with sequence comparisons that heme b_H is ligated by His70 and His155. Heme b_L would then be ligated by His28 and His113, a conclusion which is supported by the properties of cytochrome mutated at these positions. Accordingly, heme b_H in Cyt b_{558} is located close to the cytoplasmic side of the membrane where FP and IP is bound. Heme b_L is located near the outer side of the membrane, apparently close to a quinone binding site (Smirnova et al., 1995).

ACKNOWLEDGMENT

We are grateful to Karin Tsiobanelis for technical assistance and to Dr. Irina Smirnova for help with the analysis of redox data and spectra.

REFERENCES

Abraham, P. R., Mulder, A., van't Riet, J., & Raué, H. A. (1994) *Mol. Gen. Genet. 242*, 708−716.
Ackrell, B. A. C., Johnson, M. K, Gunsalus, R. P., & Cecchini, G. (1992) in *Chemistry and Biochemistry of Flavoenzymes* (Mueller, Ed.) Vol. 3, pp 229−297, CRC Press, Boca Raton, FL.
Bergström, J. (1985) *FEBS Lett. 183*, 87−90.
Cochran, B., Capaldi, R. A., & Ackrell, B. A. C. (1994) *Biochim. Biophys. Acta 1188*,162−166.
Creighton, T. E., & Freedman, R. B. (1993) *Curr. Biol. 3*, 790−793.
Daignan-Fornier, B., Valens, M., Lemire, B. D.,, & Bolotin-Fukuhara, M. (1994) *J. Biol. Chem. 269*, 15469−15472.
de Bruijn, F. J., & Lupski, J. R. (1984) *Gene 27*, 131−149.
Degli Esposti, M. (1989) *Biochim. Biophys. Acta 977*, 249−265.
Degli Esposti, M., Crimi, M., Körtner, C., Kröger, A., & Link, T. (1991) *Biochim. Biophys. Acta 1056*, 243−249.
Fortnagel, P., & Freese, E. J. (1968) *J. Bacteriol. 95*, 1431−1438.
Fridén, H., & Hederstedt, L. (1990) *Mol. Microbiol. 4*, 1045−1056.
Fridén, H., Rutberg, L., Magnusson, K., & Hederstedt, L. (1987) *Eur. J. Biochem. 168*, 695−701.
Fridén, H., Cheesman, M. R., Hederstedt, L., Andersson, K. K., & Thomson, A. J. (1990) *Biochim. Biophys. Acta 1041*, 207−215.

Gutierrez, C., Barondess, J., Manoil, C., & Beckwith J. (1987) *J. Mol. Biol. 195*, 289−297.
Hägerhäll, C. (1994) Thesis, Lund University, Lund, Sweden.
Hägerhäll, C., Aasa, R., von Wachenfeldt, C., & Hederstedt, L. (1992) *Biochemistry 31*, 7411−7421.
Haima, P., Bron, S., & Venema, G. (1987) *Mol. Gen. Genet. 209*, 335−342.
Hasnain, S., Sammons, R., Roberts, I., & Thomas, C. M. J. (1985) *J. Gen. Microbiol. 131*, 2269−2279.
Hederstedt, L. (1986) *Methods Enzymol. 126*, 399−414.
Hederstedt, L., & Rutberg, L. (1980) *J. Bacteriol. 144*, 941−951.
Hederstedt, L., & Ohnishi, T. (1992) in *Molecular Mechanisms in Bioenergetics* (Ernster, L., Ed.) pp 163−198, Elsevier, Amsterdam.
Hederstedt, L., Bergman, T., & Jörnvall, H. (1987) *FEBS Lett. 213*, 385−390.
Hoch, J. A. (1991) *Methods Enzymol. 204*, 305−320.
Ingledew, W. J., Rothery, R. A., Gennis, R. B., & Salerno, J. C. (1992) *Biochem. J. 282*, 255−259.
Kunkel, T. A., Roberts, J. D., & Zakour, R. A. (1987) *Methods Enzymol. 154*, 367−382.
Magnusson, K., Hederstedt, L., & Rutberg, L. (1985) *J. Bacteriol. 162*, 1180−1185.
Magnusson, K., Philips, M. K., Guest, J. R., & Rutberg, L. (1986) *J. Bacteriol. 166*, 1067−1071.
Maguire, J. J., Magnusson, K., & Hederstedt, L. (1986) *Biochemistry 25*, 5202−5208.
Manoil, C., & Beckwith, J. (1985) *Proc. Natl. Acad. Sci. U.S.A. 82*, 8129−8133.
Manoil, C., Mekalanos, J. J., & Beckwith, J. (1990) *J. Bacteriol. 172*, 515−518.
Phillips, M. K., Hederstedt, L., Hasnain, S., Rutberg, L., & Guest, J. R. (1987) *J. Bacteriol. 169*, 864−873.
Robertson, D. E., Farid, R. S., Moser, C. C., Urbauer, J. L., Mulholland, S. E., Pidikiti, R., Lear, J. D., Wand, A. J., DeGrado, W. F., & Dutton, P. L. (1994) *Nature 368*, 425−432.
Salerno, J. C., & Ingledew, W. J. (1991) *Eur. J. Biochem. 198*, 789−792.
Sambrook, J., Fritsch, E. F., & Maniatis, T. (1989) *Molecular Cloning*, 2nd ed., Cold Spring Harbor Laboratory Press, Cold Spring Harbor, NY.
Smirnova, I., Hägerhäll, C., Konstantinov, A. A., & Hederstedt, L. (1995) *FEBS Lett. 359*, 23−26.
Spizizen, J. (1958) *Proc. Natl. Acad. Sci. U.S.A. 44*, 1072−1078.
von Heijne, G. (1986) EMBO J. *5*, 3021−3027.
von Wachenfeldt, C. (1992) Thesis, Lund University, Lund, Sweden.
von Wachenfeldt, C., & Hederstedt, L. (1990) *FEBS Lett. 270*, 147−151.
Wood, D., Darlison, M. G., Wilde, R. J., & Guest, J. R. (1984) *Biochem. J. 222*, 519−534.
Yanisch-Perron, C., Vieira, J., & Messing, J. (1985) *Gene 33*, 103−119.
Yu, L., Wei, Y.-Y., Usui, S., & Yu, C.-A. (1992) *J. Biol. Chem. 267*, 24508−24515.
Yun, C.-H., van Doren, S. R., Crofts, A. R., & Gennis, R. B. (1991) *J. Biol. Chem. 266*, 10967−10973.